PHILOSOPHICAL TRANSACTIONS OF THE ROYAL SOCIETY B

Phil. Trans. R. Soc. B (2008) **363**, 1293–1303
doi:10.1098/rstb.2007.2226
Published online 29 October 2007

A ligand field chemistry of oxygen generation by the oxygen-evolving complex and synthetic active sites

Theodore A. Betley, Yogesh Surendranath, Montana V. Childress, Glen E. Alliger, Ross Fu, Christopher C. Cummins and Daniel G. Nocera*

Department of Chemistry, Massachusetts Institute of Technology, 77 Massachusetts Avenue, 6-335, Cambridge, MA 02139-4307, USA

Oxygen–oxygen bond formation and O_2 generation occur from the S_4 state of the oxygen-evolving complex (OEC). Several mechanistic possibilities have been proposed for water oxidation, depending on the formal oxidation state of the Mn atoms. All fall under two general classifications: the AB mechanism in which nucleophilic oxygen (base, B) attacks electrophilic oxygen (acid, A) of the Mn_4Ca cluster or the RC mechanism in which radical-like oxygen species couple within OEC. The critical intermediate in either mechanism involves a metal oxo, though the nature of this oxo for AB and RC mechanisms is disparate. In the case of the AB mechanism, assembly of an even-electron count, high-valent metal-oxo proximate to a hydroxide is needed whereas, in an RC mechanism, two odd-electron count, high-valent metal oxos are required. Thus the two mechanisms give rise to very different design criteria for functional models of the OEC active site. This discussion presents the electron counts and ligand geometries that support metal oxos for AB and RC O–O bond-forming reactions. The construction of architectures that bring two oxygen functionalities together under the purview of the AB and RC scenarios are described.

Keywords: photosynthesis; water oxidation; oxygen-evolving complex; catalysis; solar energy

1. THE NATURE OF THE Mn–OXO INTERACTION IN OEC

The bond-making and bond-breaking reactions of dioxygen in biology are managed at the metals of cofactors (Holm *et al.* 1996). Most metallocofactors use oxygen to derive their function; these include the haem iron centres of monooxygenases (Sono *et al.* 1996; Dunford 1999; Newcomb & Toy 2000; Watanabe 2000; Meunier *et al.* 2004) and the molybdenum and tungsten of oxotransferases (Kisker *et al.* 1997; Enemark *et al.* 2004) to perform substrate oxidation, the Fe–Cu centre of cytochrome *c* oxidase to drive metabolic respiration (Malmström 1990; Wikström 2004; Bertini *et al.* 2006; Busenlehner *et al.* 2006; Hosler *et al.* 2006) and copper oxidases for oxygen binding, activation and subsequent substrate oxidation (Solomon *et al.* 1996; Rosenzweig & Sazinsky 2006; Yoon & Solomon 2007). In all cases, metal oxos appear as critical intermediates in the management of oxygen. The oxo may be terminal, bound by a multiple bond to a single metal centre as in the case of haem peroxidases (Watanabe 2000; Newcomb *et al.* 2006), or the oxo may engage in single bonding to multiple metal centres, as is the case for ribonucleotide reductase (Jordan & Reichard 1998; Stubbe & van der Donk 1998; Stubbe *et al.* 2003), methane monooxygenase (Feig & Lippard 1994; Hanson & Hanson 1996; Que & Ho 1996; Wallar & Lipscomb 1996; Lieberman & Rosenzweig 2005) and galactose oxidase (Whittaker 2003), to name a few. Both binding modes may be relevant to the most important metallocofactor that is able to produce oxygen—the oxygen-evolving complex (OEC) of photosystem II (PS II). Current structural models of the OEC show oxos within the Mn_4Ca cluster singly bonded to two and three Mn centres of the core, and in the dangler model (Peloquin & Britt 2001), an oxo is proposed to be multiply bonded to the dangling Mn.

The appearance of the structures of the photosynthetic membrane (Ferreira *et al.* 2004; Loll *et al.* 2005; Yano *et al.* 2006) together with complementary structural studies of the Kok cycle (Haumann *et al.* 2005) has led to various proposals for possible mechanisms of O_2 generation. Figure 1 lists current proposals for the various electron counts of the S states of the OEC, which were proposed during the Philosophical Discussion at the Royal Society (Dutton *et al.* 2006). The O–O bond is believed to be formed in the critical S_4 state for which the least is known. The precise nature of the active site has profound consequences to the mechanism and consequently the design of catalysts for oxygen generation. If all the oxidizing equivalents are borne by the Mn centres, a $[Mn^{IV}{}_3Mn^{V}]$ core is obtained. For this model, the oxygen is activated at the 'dangler' Mn^{V} centre. A tetragonal geometry is effectively assumed for the oxo in the OEC. In this geometry, the oxo donates its orthogonal electron lone pairs to the Mn^{V} centre via the $e(d_{xz}, d_{yz})$ orbital set. The movement of electron pairs

* Author for correspondence (nocera@mit.edu).

One contribution of 20 to a Discussion Meeting Issue 'Revealing how nature uses sunlight to split water'.

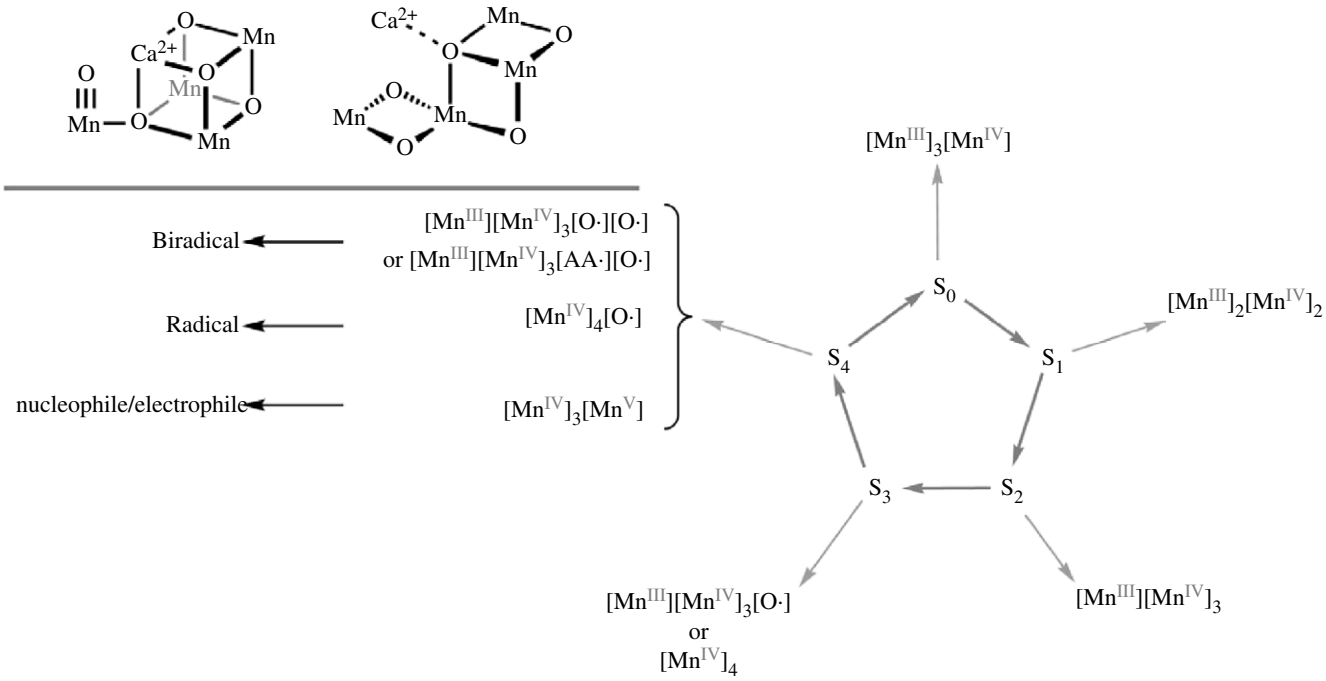

Figure 1. Current proposals for the various electron counts of the S-states of the Kok cycle.

from the oxygen to the metal centre makes the oxygen more acidic or electrophilic. Such electrophilic oxos (acids) are susceptible to attack by nucleophiles (bases). For instance, in organic reaction chemistry, this type of oxo is attacked by the two-electron bond of an olefin, thus forming the basis for catalytic oxidations (Zhang *et al.* 1990; Jacobsen *et al.* 1999; Yang *et al.* 2006; Yang & Nocera 2007). In the case of a $[Mn^{IV}{}_3Mn^{V}]$ centre, a similar mechanism is proposed with the two-electron bond of the olefin replaced by the lone pair of a hydroxide delivered from the calcium of the cofactor (McEvoy & Brudvig 2006). Alternatively, radical character has also been proposed to reside on two oxos of a $[Mn^{III}Mn^{IV}{}_3,O^{\cdot},O^{\cdot}]$ cofactor or on an oxo and amino acid of a $[Mn^{III}Mn^{IV}{}_3,O^{\cdot},AA^{\cdot}]$ (AA = amino acid) cofactor. In this case, one may envisage the O–O bond formation to occur by coupling of the biradical pair; this model gives credence to proposals of O_2 generation via peroxide-like intermediates (Ruttinger & Dismukes 1997; Siegbahn 2006). A $[Mn^{IV}{}_4,O^{\cdot}]$ core places a single-radical spin on oxygen and O_2 is generated by an undefined mechanism.

2. DIFFERENT METAL-OXO LIGAND FIELDS FOR O–O BOND FORMATION

The variegated formalisms of the OEC give rise to fundamentally different mechanisms for the O–O bond formation: acid(electrophilic)–base(nucleophilic) (AB) or radical coupling (RC). These different mechanisms call for different ligand fields in which the metal oxo resides and correspondingly *different metal-oxygen coordination environments* and *electron configurations*. Three prevailing ligand fields are shown in figure 2. Discussion of the chemistry derived from these ligand fields is based on orbital energy levels. Differing spin states for an electron count are not treated explicitly, though it is readily acknowledged that the spin state is an important determinant of the metal-oxo bond strength and reaction pathway. Moreover, secondary effects such as Jahn–Teller distortions will also perturb the overall energetics of the system. All such factors must ultimately be considered in the context of the ensuing ligand fields for the proper design of water-splitting catalysts.

(a) *Tetragonal oxo fields*

As mentioned in figure 1, a prevailing model for O_2 generation at the OEC involves an AB mechanism in which hydroxide attacks an electrophilic oxygen. The origins of the electrophilic oxygen can be found in the molecular orbital diagram shown in figure 2*b*. The diagram can be obtained by replacing an axial ligand of an ML_6 octahedral complex with an oxo. This substitution lowers the t_{2g} orbital symmetry to $b_2(d_{xy})$ and $e(d_{xz}, d_{yz})$ and the metal-ligand σ antibonding e_g orbital symmetry to $b_1(d_{x^2-y^2})$ and $a_1(d_{z^2})$ levels. Because the metal-oxo bond is short, the d_{z^2} orbital is more destabilized than in its ML_6 parent. Similarly, the $e(d_{xz}, d_{yz})$ orbitals are destabilized relative to their octahedral parentage because they are π antibonding with respect to the oxygen $2p_x$ and $2p_y$ orbitals. Owing to the prevalence of these σ and π interactions of the oxo with the metal, the axial ligand opposite the oxo is significantly weakened or typically absent.

The tetragonal environment (C_4 symmetry) described by figure 2*b* poises a lowest unoccupied molecular orbital (LUMO) directed along the metal-oxo axis for attack by an incoming hydroxide. This situation favours O–O bond formation. From an orbital perspective, an orbital of σ character on the hydroxide (highest occupied molecular orbital) approaches the M–O π^* orbital (LUMO). The combination leads to the formation of an O–O σ bond while breaking one of the M–O π bonds, representing a formal $2e^-$ reduction of the metal centre. The AB mechanism effectively requires an even electron system where two electron

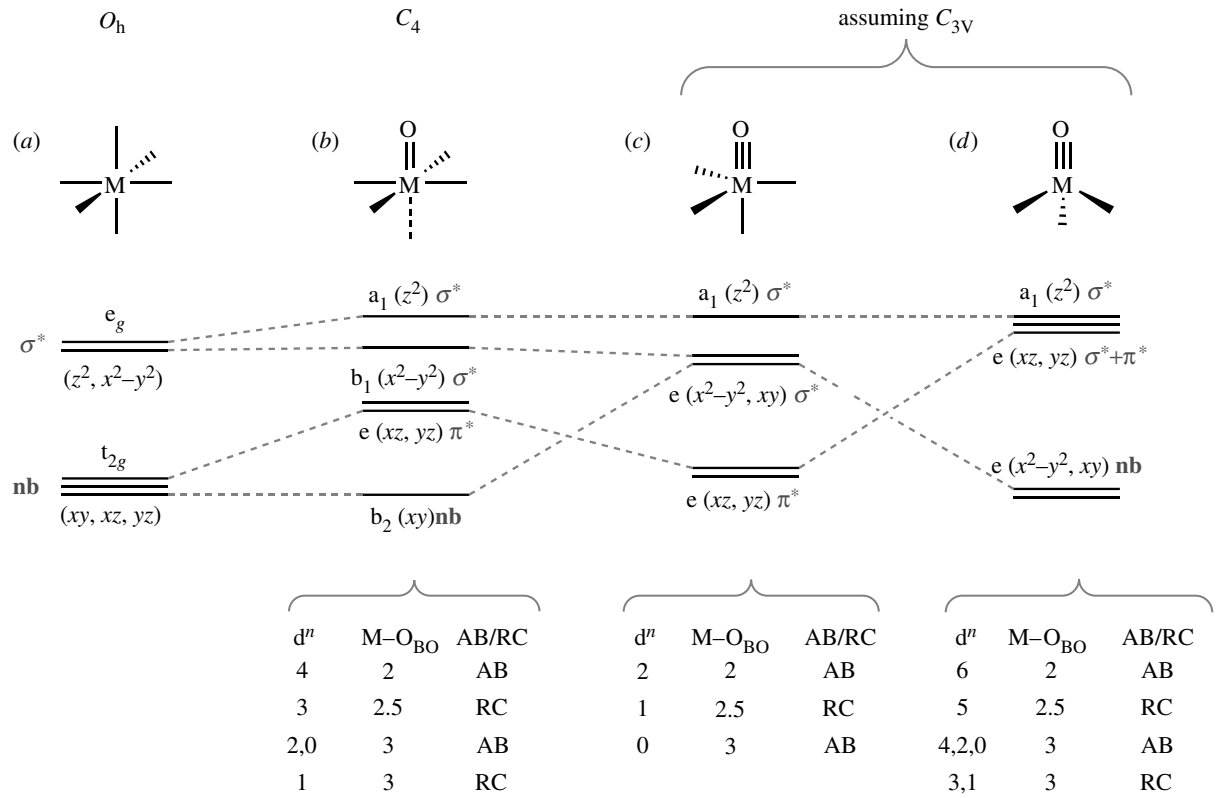

d^n	$M-O_{BO}$	AB/RC
4	2	AB
3	2.5	RC
2,0	3	AB
1	3	RC

d^n	$M-O_{BO}$	AB/RC
2	2	AB
1	2.5	RC
0	3	AB

d^n	$M-O_{BO}$	AB/RC
6	2	AB
5	2.5	RC
4,2,0	3	AB
3,1	3	RC

Figure 2. Qualitative frontier molecular orbital splitting diagrams for (*a*) an octahedral metal complex and a metal oxo residing in a (*b*) tetragonal field, (*c*) trigonal bipyramidal and (*d*) tetrahedral ligand field. The table shows the d-electron count that supports a multiple metal oxo bond and the preferred mechanism for the O–O bond coupling, where AB is acid/base and RC, radical coupling. Only low-spin configurations are considered. The assignment of AB and RC will change with high-spin configurations.

holes of the (d_{xz}, d_{yz}) LUMO of a d^4 metal oxo are filled by the attacking electron pair of the hydroxide. Alternatively, a d^2 metal oxo is even more electrophilic as the LUMO is completely unoccupied and hence even more acidic than the partially occupied LUMO of the d^4 metal centre. As of now, how the overall spin state of the metal-oxo precursor and its correlation to products determines the reaction kinetics remains undefined. We note that the AB mechanism can be considered the microscopic reverse of the O–O bond heterolysis step in cytochrome P450 to produce H_2O and a ferryl (Denisov *et al.* 2005; Shaik *et al.* 2005). In this problem, the effect of spin has been accounted for computationally. Similar treatments for the O–O bond-forming reaction are warranted.

The same tetragonal ligand field can support an RC mechanism but for a different electron count. Population of the degenerate e(d_{xz}, d_{yx}) level of the metal oxo with a single electron results in a singly occupied molecular orbital. Thus a d^3 metal centre gives rise to the radical character of the metal-oxo moiety. Note, for a d^5 centre, most of the metal-oxo π-bonding is lost (formally only 0.5 π bond is preserved) owing to the three-electron occupancy of the e(d_{xz}, d_{yz}) set, which is metal-oxo π^* in character. Accordingly, a terminal d^5 oxo is difficult to attain in a tetragonal field. The precise location of the radical in the d^3 case—metal versus oxygen centred—depends largely on the nature of the metal-oxo interaction. For the most part, the issue of the extent of oxygen radical character at odd-electron metal-oxo centres has remained experimentally unresolved.

Though in the same ligand field, the AB and RC mechanisms give rise to drastically different catalyst design criteria. The O–O bond formation for the AB mechanism requires the assembly of a high-valent oxo in a tetragonal ligand field and a hydroxide, whereas O–O bond formation for the RC mechanism requires the assembly of two high-valent metal oxos in tetragonal fields. This aspect of disparate design for tetragonal metal-oxo moieties will be addressed in §3.

(b) *Trigonal oxo fields*

The radicals of an RC mechanism are supported by the local C_3 symmetry of a metal oxo in a trigonal environment. When an axial ligand is present (the trigonal bipyramidal case shown in figure 2*c*), the orbital splitting pattern from lowest to highest energy is a degenerate level comprising the d_{xz} and d_{yz} orbitals, another degenerate level formed from the $d_{x^2-y^2}$ and d_{xy} orbitals and a highest energy d_{z^2} orbital. The $d_{x^2-y^2}$ and d_{xy} orbitals rise above the d_{xz} and d_{yz} orbitals because the former take on substantial M–L σ^* character and thus are destabilized. For a d^4 case, the LUMO is $d_{x^2-y^2}$ and d_{xy} and the π bonds are annihilated owing to the $4e^-$ occupancy of the M–O π^* e(d_{xz}, d_{yz}) set. Consequently, the terminal metal oxo is inaccessible to d^4 metals in a trigonal bipyramidal ligand field. For the d^2 electron count, two electrons occupy a degenerate e(d_{xz}, d_{yz}) orbital level. Thus, this system, from an electronic perspective, looks very much like a metal oxo in a tetragonal field with a d^4 electron count (vide infra). For the d^0 case, the e(d_{xz}, d_{yz}) orbital set is empty and akin to

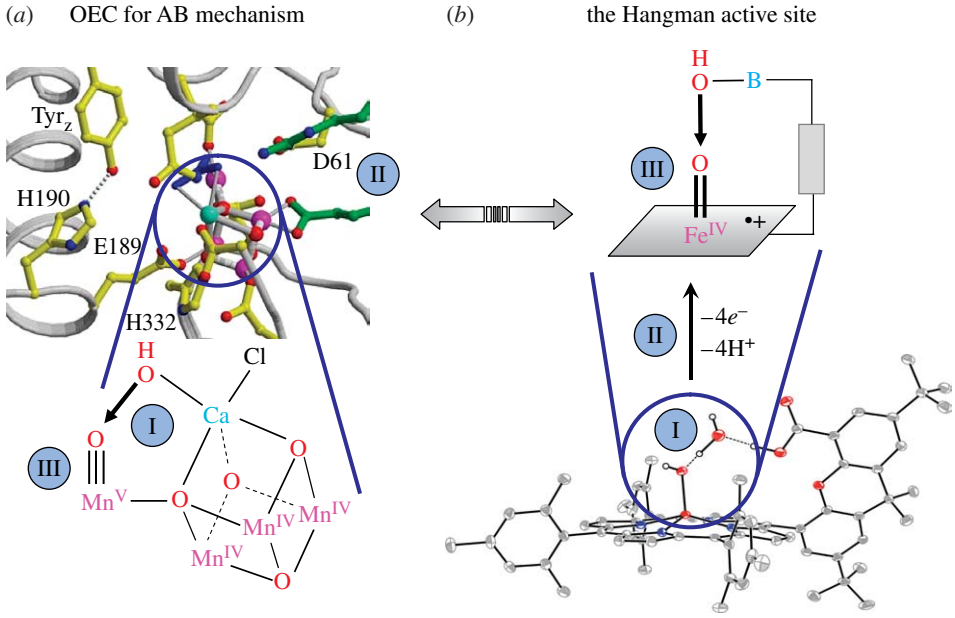

Figure 3. (*a*) The water oxidation centre in photosystem II (Ferreira *et al.* 2004) and (*b*) the Hangman porphyrin (I) assemble the oxygen of two waters for coupling, (II) activate the water to oxo by PCET and (III) position a high-valent oxo along the reactive metal hydroxide vector. Though the resting state of the Hangman is a Fe^{III}–$OH\cdots H_2O$ complex, the Hangman porphyrin is prepared by the introduction of an Fe^{II} into the porphyrin core and the assembly of two waters. Production of the Compound I intermediate of the Hangman thus results from an overall ($4e^-$,$4H^+$) process.

the case of a d^2 electron count of a metal oxo in a tetragonal field. As with the d^2/d^4 even-electron systems of the tetragonal field, a metal oxo with a d^0/d^2 electron count in a trigonal bipyramidal field lends itself to O–O bond formation by an AB mechanism. More generally, for low electron counts, $d^n(M–O)_{tetra} \sim d^{n-2}(M–O)_{tbp}$. This analogy holds for the odd-electron count as well: $d^1(M–O)_{tbp}$ and $d^3(M–O)_{tbp}$ are similar to $d^3(M–O)_{tetra}$ and $d^5(M–O)_{tetra}$, respectively. For the same reasons mentioned for a $d^5(M–O)_{tetra}$ centre, the $d^3(M–O)_{tbp}$ centre has a 0.5 π bond order, and thus it is fragile and difficult to realize. The d^1 system, however, presents a robust metal oxo with putative radical character and accordingly the system lends itself to O–O bond formation by an RC mechanism.

(c) *Tetrahedral ligand fields*

Metals with higher d-electron counts can exhibit AB and RC oxo reactivity if the apical ligand opposite the metal-oxo vector of the trigonal bipyramid is removed to attain the local coordination environment of a pseudo-tetrahedron. The d-orbital diagram obtained for this metal-oxo ligand coordination geometry is shown in figure 2*d*. The metal-based orbitals involved in the σ and π M–O interactions are the highest in energy owing to their antibonding character. The ordering of the $a_1(d_{z^2}(\sigma^*))$ and $e(d_{xz}, d_{yz}(\pi^*))$ depends on the tridentate ligand's bite angle (Jenkins *et al.* 2002). The distinguishing trait of the application of this ligand field to the metal oxo is that a degenerate $e(d_{x^2-y^2}, d_{xy})$ level is lowest in energy and may accommodate up to four electrons in a low-spin configuration before the metal π^* orbitals are populated. Hence, late transition metals may be used to effect AB (metals of even electron counts, d^4 and possibly d^6) and RC (metals of odd electron count, d^5) O–O bond-forming mechanisms. Moreover, high-spin states are likely to be accessible, and thus might be used resourcefully to activate the metal-oxo bond. Targeting this framework, therefore, in principle will allow chemists to design mid-to-late transition metal platforms that are amenable to high oxidation states, but will tolerate higher d-electron counts in a parent complex without destabilization of the M–O linkage.

3. EXPERIMENTAL REALIZATION OF METAL–OXO COFACTORS IN DIFFERENT LIGAND FIELDS

Approaches to the design of catalysts possessing the metal-oxo cofactor within the ligand fields described by figure 2 are now presented.

(a) *Metal-oxo cofactors in tetragonal fields*

(i) *AB mechanism*

Figure 3*a* shows the structure of the OEC active site that is consistent with an AB mechanism. The key intermediate in the critical bond-forming step of water oxidation is a pre-organized oxo/hydroxyl intermediate. The Ca^{2+} ion is thought to decrease the pK_a of a bound water to produce a nucleophilic hydroxide in the secondary coordination sphere that attacks the electrophilic oxo of a high-valent manganese (Messinger *et al.* 1995; Pecoraro *et al.* 1998; Vrettos *et al.* 2001). The challenges confronting the development of a functional model for O_2 generation by the AB mechanism at the OEC are labelled in figure 3:

(I) Active sites must permit control of the secondary coordination environment such that two water molecules may be pre-assembled for the O–O bond coupling.
(II) Water must be activated by coupling proton transfer reactions to electron transfer. The removal of electrons and protons at the OEC

active site finds its origins in the Kok cycle (Westphal *et al.* 2000; Tommos 2002; Haumann *et al.* 2005). Proton-coupled electron transfer (PCET) activation of the substrate may be managed by a proton exit channel beginning at the D61 residue (Barber 2006).

(III) The high-valent metal oxo must be generated for attack by the water-derived hydroxide.

We have tackled the challenges presented by (I)–(III) by constructing 'Hangman' platforms (Yeh *et al.* 2001; Chng *et al.* 2003). The Hangman structure assembles water molecules (challenge I) by using a scaffold to 'hang' one water molecule over another that is coordinated to the Fe(III) centre of a haem platform. Figure 3*b* shows the crystal structure of Hangman porphyrin (Yeh *et al.* 2001). A carboxylic acid group appended to a xanthene scaffold suspends an exogenous water molecule in the Hangman cleft via hydrogen bonding. The binding energy of the water molecule is 5.8 kcal mol^{-1} (Chang *et al.* 2003) and its association within the cleft is reversible. The Hangman's pendant mimics the amino acid residues that orient water in the distal cavities of haem peroxidases by precisely positioning an acid–base functional group over the face of the haem. We have since generalized the Hangman approach to include salen macrocycles (Liu & Nocera 2005). As with haem peroxidases, the Hangman platform supports an electrophilic oxo (challenge III) of the Compound I (Cpd I; De Montellano 1995; Sono *et al.* 1996; Dunford 1999; Watanabe 2000; Newcomb *et al.* 2006) type, which is two redox levels above Fe^{III} with a ferryl $Fe^{IV}=O$ residing within an oxidized porphyrin π-radical cation, $P^{\cdot+}$. The electrophilic oxo has been observed by cryogenic stopped-flow spectroscopy (Soper *et al.* 2007). The production of the oxo is derived from the ability of the Hangman to perform PCET (challenge II; Liu & Nocera 2005; Hodgkiss *et al.* 2006; Yang *et al.* 2006; Soper *et al.* 2007; Yang & Nocera 2007). The importance of the PCET mechanism in the activation of water and other small molecules has been presented in a recent Philosophical Society Discussion (Reece *et al.* 2006). In short, the pendent H^+ donor group in the Hangman system exerts control over the PCET production of the electrophilic oxo from peroxide intermediates by coupling PT to internal $2e^-$ redox events of the redox (salen or porphyrin) cofactor (Yang *et al.* 2006; Rosenthal *et al.* 2007; Soper *et al.* 2007; Yang & Nocera 2007). As with haem peroxidases, the electrophilic oxo, $P^{\cdot+}Fe^{IV}=O$, is susceptible to attack by nucleophiles such as two electrons of the π-bond of olefins (Yang & Nocera 2007). The goal now is to see whether the oxo is sufficiently electrophilic to be attacked by hydroxide. If not, the porphyrin will be modified with electron-withdrawing groups such as pentafluorinated phenyls in the meso positions with the aim of increasing the electrophilicity of the $Fe^{IV}=O$.

The similarities of a potential $[Mn^{IV}{}_3Mn^{V}]$ S_4 state of OEC and the Hangman system are highlighted in figure 3. Both centres assemble two water molecules within a cleft. An electrophilic oxo in a tetragonal ligand may be produced at either centre by PCET. For the case of the proposed model for the S_4 state of OEC, the oxo is bonded to a d^2 centre of Mn(V), whereas for the Hangman cofactor, the oxo is bonded to a d^4 metal centre of Fe(IV). Both OEC and the Hangman porphyrins possess a proximate site to deliver hydroxide (from the Ca^{2+} in OEC and from the hanging group in Hangman) to the oxo, which is susceptible to nucleophilic attack. But in the case of the Hangman cofactor, the use of hydroxide as the nucleophile remains to be demonstrated.

(ii) *RC mechanism*

Meyer's (Gersten *et al.* 1982) blue dimer complex $[(bpy)_2(OH_2)Ru^{III}(\mu\text{-}O)Ru^{III}(OH_2)(bpy)_2]^{4+}$ (**1** in figure 4) catalyses the oxidation of water to molecular oxygen at 1.4 V versus normal hydrogen electrode (NHE; pH 1) with 10–25 turnovers. This species is composed of a dimeric ruthenium core connected by a nearly linear μ-oxo bridge. Kinetic analysis reveals that the initial $[(OH_2)Ru^{III}(\mu\text{-}O)Ru^{III}(OH_2)]$ core undergoes a series of coupled proton and electron transfers to produce a $[(O)Ru^{V}(\mu\text{-}O)Ru^{V}(O)]$ species that precedes O–O bond formation (Binstead *et al.* 2000). Although there remains much mechanistic uncertainty over the nature of the discrete mechanism by which the O–O bond formation occurs, the precursor to oxygen formation is two d^3 metal oxos in tetragonal ligand fields disposed in a side-by-side orientation. From the perspective of figure 2*b*, the odd-electron system may be formulated as side-by-side oxo radical centres, though their direct coupling has not been implicated as a dominant reaction pathway. Structural and electronic features unique to the blue dimer and related analogues (Sens *et al.* 2004; Zong & Thummel 2005) indeed inhibit a straightforward RC reaction path. Geometric constraints imposed by the ancillary ligands and the μ-oxo bridge prevent oxygen atoms from attaining the correct geometry to form an O–O bond. It has been estimated that rotation about the μ-O bond to yield an eclipsed geometry of the M–O vectors still places the O atoms 3.2 Å apart (Gilbert *et al.* 1985). Coupling at this distance would require a significant distortion or the participation of water to mediate the radical coupling. In addition, putative radical character may be diminished by antiferromagnetic coupling through the μ-O bridge (Yang & Baik 2004, 2006).

In the light of these barriers to an RC mechanism, we have designed the Pacman systems of figure 4 (**2** and **3**) to remove impediments to RC while largely retaining the d^3 oxo character of the blue dimer system. The Pacman complexes use dimethylxanthene (DTX; **2**) and dibenzofuran (DPD; **3**) organic spacers to connect two tridentate terpyridine ligands. These organic scaffolds have been previously applied to create cofacially oriented Pacman porphyrins (Chang *et al.* 2000*a*,*b*, 2002*a*,*b*; Deng *et al.* 2000). In the Pacman approach, the two Ru oxos are oriented towards each other to enable their direct interaction. Moreover, the oxo centres are electronically isolated from each other by imposing the long covalent pathway between them via the scaffold. We have shown that the Pacman scaffolds are flexible enough to accommodate over a four-angstrom range in metal–metal distance (Deng *et al.* 2000). We envision that this flexibility would allow the metal centres to clamp down, facilitating O–O coupling, while retaining the ability to spring open, release O_2 and bind water. Electrochemical studies indicate that the Pacman

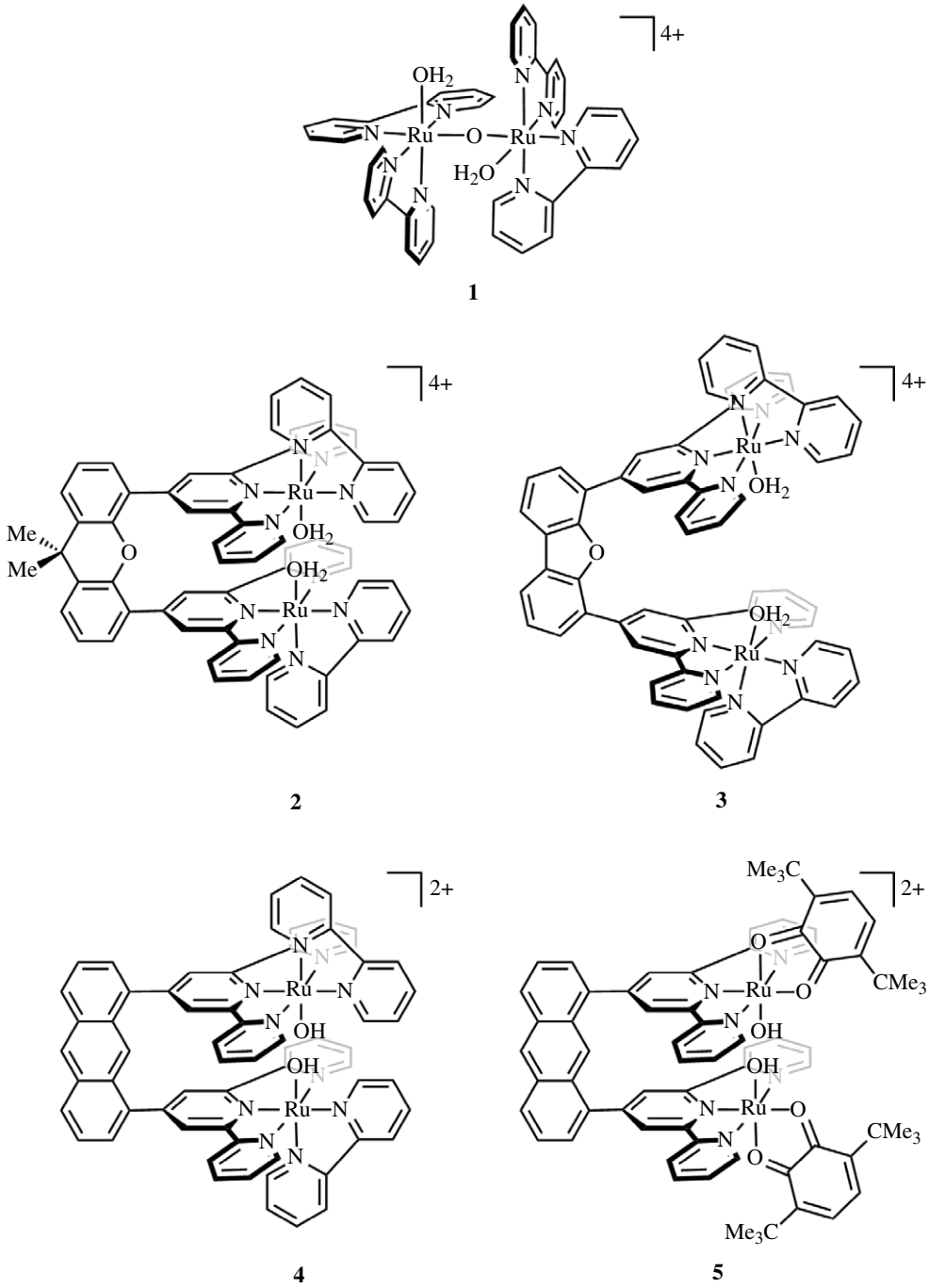

Figure 4. Bimetallic ruthenium compounds capable of water splitting: Meyer's blue oxo dimer complex $[(bpy)_2(OH_2)Ru^{III}(\mu\text{-}O)Ru^{III}(OH_2)(bpy)_2]^{4+}$ (**1**) and cofacial diruthenium platforms on the scaffolds of dimethylxanthene (**2**), dibenzofuran (**3**) and anthracene (**4**,**5**).

complexes are stable through the range of oxidation states of Ru^{II} to $Ru^{IV}(O)$, in contrast to the analogous blue dimer fragment that is unstable towards disproportionation. Further oxidation of the $Ru^{IV}(O)$ at 1.4 V versus Ag/AgCl (pH = 7) for both the DTX (**2**) and DTD (**3**) systems leads to oxygen production, which has been verified by a standard pyrogallol analysis. The mechanism of oxygen production is currently under study. It is noteworthy that the monomeric Ru centres are inert for water oxidation to O_2 (McHatton & Anson 1984; Takeuchi *et al.* 1984). Our observations of the DTX and DTD Pacman complexes agree with those obtained for Pacman complexes employing an anthracene spacer between the Ru terpyridine centres (Wada *et al.* 2001*a*,*b*). These coordination spheres are completed by either a bipyridine (**4**, figure 4) or a 3,6-di-*tert*-butyl-1,2-benzoquinone (**5**, figure 4) ligand. Interestingly, the bipyridine complex is reported to exhibit modest activity for O_2 production at potentials beyond 1.31 V. Conversely, the introduction of the redox-active benzoquinone ligand in **5** (figure 4) leads to a pronounced increase in O_2 production. The reasons for this enhanced activity of Ru Pacman systems possessing redox-active, ancillary ligands are unknown.

(**b**) *Metal-oxo cofactors in trigonal bipyramidal fields*

As shown in figure 2*c*, the lowest lying metal-based orbital for a metal oxo in a trigonal bipyramidal field is a degenerate level composed primarily of the d_{xz}

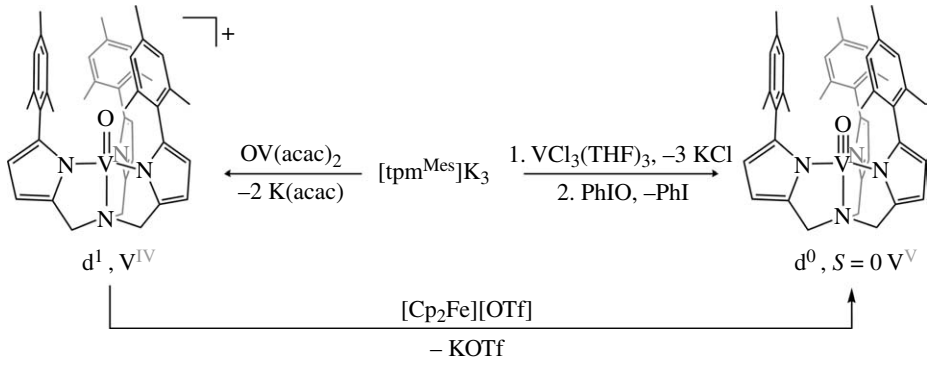

Figure 5. The trigonal bipyramidal field offered by the tris(pyrrolide)amine framework. The complex is stabilized for the oxo complexes of V^{IV} and V^{V} formal oxidation states.

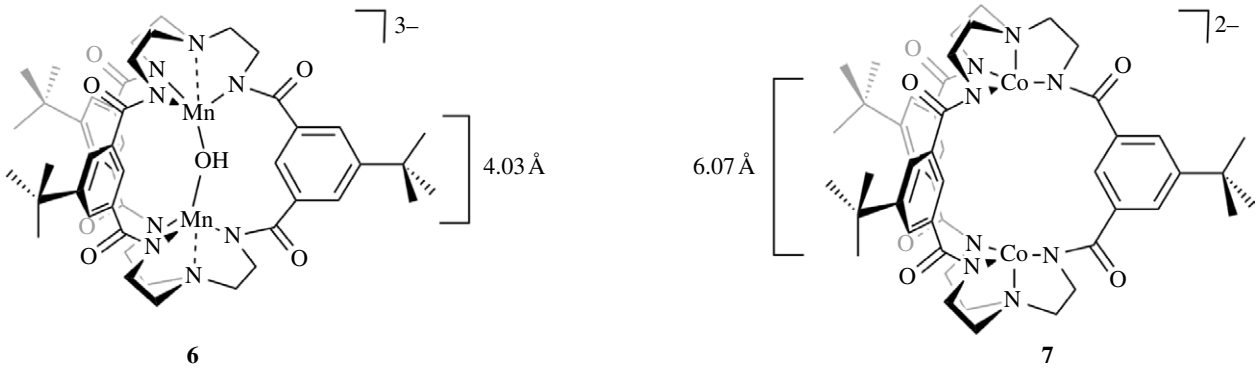

6 **7**

Figure 6. Hexaanionic cryptands to support the coupling of two high-valent oxos by an RC mechanism.

and d_{yz} orbitals. This limits the stabilization of the metal-oxo multiple bond to metals with a d^0 or d^1 configuration. To test the limit of oxo stability in this geometry, we have created the modified tris(pyrrolyl-α-methyl)amine framework (Betley & Nocera submitted *a*) shown in figure 5 to survey group V oxo chemistry. The ligand design is based on Odom's parent scaffold (Shi *et al.* 2004). Substitution of 2-arylpyrroles (Rieth *et al.* 2004) for pyrrole in Odom's reported synthesis produces the target tris(pyrrolyl-α-methyl)amine ligand in high yields (aryl=mesityl). A family of V^{IV} species and V^{V} oxo complexes have been synthesized that uses this ligand framework. The trigonally coordinated $V(mesityl)_3$ readily condenses with single O-atom bridges to form V^{IV} species $[(mesityl)_3V^{IV}]_2(\mu\text{-O})$ (Odom & Cummins 1995). The large aryl substituents of the ligand framework block the μ-oxo dinuclear structure from forming. Currently, the terminal oxo of V^{IV} (d^1) has been targeted to probe where the radical character largely resides, i.e. on the metal or the oxygen.

Appearance of radical character at the oxygen of the $(M–O)_{tbp}$ centre is critical to advancing the RC mechanism for O–O bond coupling. However, this criterion alone is insufficient. The trigonal bipyramidal scaffold needs to be elaborated so that two oxos may be brought together for coupling. We have set out on a course of study to address this challenge with the synthesis of the cryptands shown in figure 6. The active site combines the features of the TREN-based (TREN=tris(2-aminoethyl)amine) metal-binding site (Schrock 1997) and the neutral hexacarboxamide cryptand (Kang *et al.* 2003). These ligands proffer a trigonal monopyramidal coordination site for the metal ions in high oxidation states, engendered by the trianionic charge of the deprotonated TREN ligand. The ligands are diametrically positioned by attaching three carboxamide *meta*-phenyl spacers between the TREN metal-binding sites. The design results in the formation of a cavity that can accommodate two high-valent metal centres in a cofacial geometry. Manganese and cobalt have been introduced into the cavity; the molecules shown in figure 6 have been structurally characterized (Alliger *et al.* in preparation). A comparison of the two structures shed light on the nature of the cavity created by the hexacarboxamido ligand. The Mn complex (figure 6, **6**) possesses a hydroxide ligand that imposes a Mn–Mn distance of 4.058 Å. With the absence of a bridging ligand, the metals relax to a Co–Co distance of 6.073 Å (figure 6, **7**). The flex in the cavity results from rotation about the metal–amide bond, which allows the ligand to bring the metal centres together in an accordion-like motion. The new ligand thus has several attributes pertaining to an RC mechanism: it (i) presents binding sites that can accommodate high-valent metal centres, a necessity for a trigonal bipyramidal ligand geometry; (ii) permits the assembly of two metal oxos within the cavity in a convergent orientation; and (iii) possesses a cavity able to flex over 2 Å, thus allowing oxos to be brought together for their subsequent RC. Moreover, the use of carboxamide linkers should render these ligands resistant to oxidation, thus avoiding ligand degradation by reactive oxygen intermediates. Current efforts are indeed focused at generating high-valent oxos within the cavity of the new ligand.

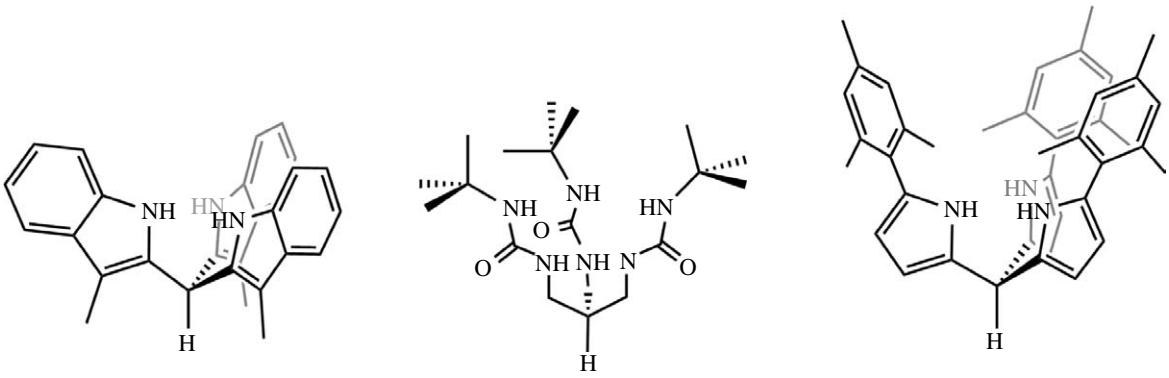

Figure 7. Trianionic platforms to support high-valent, late transition metal-oxo cores in a tetrahedral ligand field.

(c) *Metal-oxo cofactors in tetrahedral fields*

The cryptands of §4 sterically shield the metal-oxo radical species from deleterious reactivity and proximally orient the two metal-oxo vectors. The trigonal bipyramidal approach, however, does not favour metal-oxo species with d-electron counts exceeding d^2. Thus, targeting pseudo-tetrahedral frameworks will allow us, in principle, to stabilize and probe both AB and RC mechanistic possibilities with high-valent, mid-to-late transition metal ions with up to six d electrons (figure 2*d*).

The ligand scaffold for a tetrahedral field should be (i) C_3-symmetric and trianionic to achieve the desired oxidation states for the metal-oxo complexes, (ii) modular such that the steric protection about the oxo moiety can be tempered for isolation or promotion of bimolecular AB and RC reactions, (iii) oxidatively robust such that the redox events are localized within the metal-oxo framework without deleterious ligand oxidation events, and (iv) ultimately protolytically insensitive, as the desired reaction medium involves water as a substrate. We have synthesized a library of tridentate scaffolds (Betley & Nocera submitted *b*); figure 7 illustrates select platforms. They include the known tris(3-methylindolyl)methane ligand (**8**), which has been suitably employed to stabilize main group elements in the +3 oxidation state (Müller & Pindur 1984; Barnard & Mason 2001), a tris(*tert*-butylurea)methane species (**9**) evocative of platforms synthesized by Borovik (MacBeth *et al.* 2000; MacBeth *et al.* 2004), and a tris(2-mesitylpyrrolyl)methane ligand (**10**) that presents a sterically shielded trigonal environment for the metal ions. Because the target metal ion species involve mid-to-late transition elements, the trianionic ligand platforms are chosen because the N-donor basicity is attenuated by their pendent organic moiety, that is the indole, urea and pyrrole frameworks. With this library of ligand platforms in hand, investigations of the transition metal-oxo chemistry engendered by this ligand field may now be explored. These studies are currently underway.

4. SUMMARY AND OUTLOOK

The realization of a water-splitting catalyst addresses one of the greatest challenges facing our planet in the coming century—the development of a clean and renewable fuel source (Eisenberg & Nocera 2005; Lewis & Nocera 2006; Nocera 2006). The combination of water and light from the Sun can be used to produce hydrogen and oxygen. The blueprint for accomplishing this solar energy conversion is provided by photosynthesis, which converts sunlight into a wireless current which in turn is captured cathodically by photosystem I to reduce the protons to 'hydrogen' (i.e. NADPH) and anodically by OEC to produce oxygen. It is this latter transformation that poses the greatest difficulty to duplicating photosynthesis outside of the leaf.

The various proposals for the redox equivalency of the S_4 state of the Mn_4Ca cluster lead to different mechanisms for O–O bond coupling and O_2 generation. Current models of the OEC suggest the prevalence of either acid–base or radical-coupling pathways. The AB mechanism requires an electrophilic oxo for bond formation with an exogenous oxygen nucleophile. To attain such an acidic oxygen, the lone pairs of the oxo donate into empty d-orbitals of a high-valent metal to form a double or triple metal-oxo bond. We note, however, that the formation of such strong bonds imposes kinetic barriers, since the multiple metal-oxo bond must ultimately be broken for O_2 release. To this end, the AB mechanism hinges on the balance between a strong metal-oxo bond to ensure electrophilicity but it must be weak enough to allow it to be broken with facility. The participation of high-spin states in the OEC complex may provide a resolution to this quandary. Alternatively, the coupling of oxygen radicals may circumvent the requirements for a strong metal-oxo bond. Oxygen radicals may be supported by single or multiple bonds to metals in the mid-to-late transition series. The open questions surrounding the mechanism for O_2 production by the OEC provides an imperative for the design of metal oxos in coordination environments that permit the full range of stereoelectronic factors associated with O–O bond coupling to be explored. Thus it is a task for the synthetic chemist to design new ligand environments that capitalize on the discovery of OEC structure and function. Whereas an alternative approach might be pursued with solid-state materials and surfaces, a molecular approach lends itself better to mechanistic analysis. We report here progress towards this end.

The National Science Foundation supported this work with a Chemical Bonding Center grant CHE-0533150. We also acknowledge support from the Department of Energy, DOE DE-FG02-05ER15745. Y.S. thanks the DoD for a NDSEG pre-doctoral fellowship and T.A.B. thanks the NIH for a post-doctoral research fellowship.

REFERENCES

Alliger, G. E., Breiner, B., Fu, R., Cummins, C. C. & Nocera, D. G. In preparation. Dimanganese (II) and dicobalt (II) cryptates supported by a hexaanionic cryptand ligands.

Barber, J. 2006 Photosystem II: an enzyme of global significance. *Biochem. Soc. Trans.* **34**, 619–631. (doi:10.1042/BST0340619)

Barnard, T. S. & Mason, M. R. 2001 Synthesis, structure, and coordination chemistry of the bicyclic π-acid phosphatri(3-methylinolyl)methane. *Organometallics* **20**, 206–214. (doi:10.1021/om000793y)

Bertini, I., Cavallaro, G. & Rosato, A. 2006 Cytochrome *c*: occurence and functions. *Chem. Rev.* **106**, 90–115. (doi:10.1021/cr050241v)

Betley, T. A. & Nocera, D. G. Submitted *a*. Metal complexes supported by the tris(2-mesityl-pyrrolyl-α-methyl)amine ligand.

Betley, T. A. & Nocera, D. G. Submitted *b*. Design criteria for O–O bond formation via metal oxo complexes.

Binstead, R. A., Chronister, C. W., Ni, J., Hartshorn, C. M. & Meyer, T. J. 2000 Mechanism of water oxidation by the μ-oxo dimer $[(bpy)_2(H_2O)Ru^{III}ORu^{III}(OH_2)(bpy)_2]^{4+}$. *J. Am. Chem. Soc.* **122**, 8464–8473. (doi:10.1021/ja993235n)

Busenlehner, L. S., Salomonsson, L., Brzezinski, P. & Armstrong, R. N. 2006 Mapping protein dynamics in catalytic intermediates of the redox-driven proton pump cytochrome *c* oxidase. *Proc. Natl Acad. Sci. USA* **103**, 15 398–15 403. (doi:10.1073/pnas.0601451103)

Chang, C. J., Deng, Y., Heyduk, A. F., Chang, C. K. & Nocera, D. G. 2000*a* Xanthene-bridged cofacial bisporphyrins. *Inorg. Chem.* **39**, 959–966. (doi:10.1021/ic990987+)

Chang, C. J., Deng, Y., Shi, C., Chang, C. K., Anson, F. C. & Nocera, D. G. 2000*b* Electrocatalytic four-electron reduction of oxygen to water by a highly flexible cofacial cobalt bisporphyrin. *Chem. Commun.*, 1355–1356. (doi10.1039/b001620i)

Chang, C. J., Baker, E. A., Pistorio, B. J., Deng, Y., Loh, Z.-H., Miller, S. E., Carpenter, S. D. & Nocera, D. G. 2002*a* Structural, spectroscopic, and reactivity comparison of xanthene- and dibenzofuran-bridged cofacial bisporphyrins. *Inorg. Chem.* **41**, 3102–3109. (doi:10.1021/ic0111029)

Chang, C. J., Yeh, C. Y. & Nocera, D. G. 2002*b* Porphyrin architectures bearing functionalized xanthene spacers. *J. Org. Chem.* **67**, 1403–1406. (doi:10.1021/jo016095k)

Chang, C. J., Chng, L. L. & Nocera, D. G. 2003 Proton-coupled O–O activation on a redox platform bearing a hydrogen-bonding scaffold. *J. Am. Chem. Soc.* **125**, 1866–1876. (doi:10.1021/ja028548o)

Chng, L. L., Chang, C. J. & Nocera, D. G. 2003 Catalytic O–O activation chemistry mediated by iron Hangman porphyrins with a wide range of proton-donating abilities. *Org. Lett.* **5**, 2421–2424. (doi:10.1021/ol034581j)

De Montellano, P. R. O. (ed.) 1995 *Cytochrome P-450 structure, mechanism and biochemistry*, 2nd edn. New York, NY: Plenum Press.

Deng, Y., Chang, C. J. & Nocera, D. G. 2000 Direct observation of the 'pac-man' effect from dibenzofuran-bridged cofacial bisporphyrins. *J. Am. Chem. Soc.* **122**, 410–411. (doi:10.1021/ja992955r)

Denisov, I. G., Makris, T. M., Sligar, S. G. & Schlichting, I. 2005 Structure and chemistry of cytochrome P450. *Chem. Rev.* **105**, 2253–2277. (doi:10.1021/cr0307143)

Dunford, H. B. 1999 *Heme peroxidases*. New York, NY: Wiley.

Dutton, P. L., Munro, A. W., Scrutton, N. S. & Sutcliffe, M. J. 2006 Quantum catalysis in enzymes: beyond the transition state theory paradigm. *Phil. Trans. R. Soc. B* **361**, 1293–1455. (doi:10.1098/rstb.2006.1879)

Eisenberg, R. & Nocera, D. G. 2005 Overview of the forum on solar and renewable energy. *Inorg. Chem.* **44**, 6799–6801. (doi:10.1021/ic058006i)

Enemark, J. H., Cooney, J. J. A., Wang, J.-J. & Holm, R. H. 2004 Synthetic analogues and reaction systems relevant to the molybdenum and tungsten oxotransferases. *Chem. Rev.* **104**, 1175–1200. (doi:10.1021/cr020609d)

Feig, A. L. & Lippard, S. J. 1994 Reactions of non-heme iron(II) centers with dioxygen in biology and chemistry. *Chem. Rev.* **94**, 759–805. (doi:10.1021/cr00027a011)

Ferreira, K. N., Iverson, T. M., Maghlaoui, K., Barber, J. & Iwata, S. 2004 Architecture of the photosynthetic oxygen-evolving center. *Science* **303**, 1831–1838. (doi:10.1126/science.1093087)

Gersten, S. W., Samuels, G. J. & Meyer, T. J. 1982 Catalytic oxidation of water by an oxo-bridged ruthenium dimer. *J. Am. Chem. Soc.* **104**, 4029–4030. (doi:10.1021/ja00378a053)

Gilbert, J. A., Eggleston, D. S., Murphy Jr, W. R., Geselowitz, D. A., Gersten, S. W., Hodgson, D. J. & Meyer, T. J. 1985 Structure and redox properties of the water-oxidation catalyst $[(bpy)_2(OH_2)RuORu(OH_2)(bpy)_2]^{4+}$. *J. Am. Chem. Soc.* **107**, 3855–3864. (doi:10.1021/ja00299a017)

Hanson, R. S. & Hanson, T. E. 1996 Methanotrophic bacteria. *Microbiol. Rev.* **60**, 439–471.

Haumann, M., Liebisch, P., Muller, C., Barra, M., Grabolle, M. & Dau, H. 2005 Photosynthetic O_2 formation tracked by time-resolved X-ray experiments. *Science* **310**, 1019–1021. (doi:10.1126/science.1117551)

Hodgkiss, J. M., Damrauer, N. H., Pressé, S., Rosenthal, J. & Nocera, D. G. 2006 Electron transfer driven by proton fluctuations in a hydrogen-bonded donor–acceptor assembly. *J. Phys. Chem. A* **110**, 18 853–18 858.

Holm, R. H., Kennepohl, P. & Solomon, E. I. 1996 Structural and functional aspects of metal sites in biology. *Chem. Rev.* **96**, 2239–2314. (doi:10.1021/cr9500390)

Hosler, J. P., Ferguson-Miller, S. & Mills, D. A. 2006 Energy transduction: proton transfer through the respiratory complexes. *Annu. Rev. Biochem.* **75**, 165–187. (doi:10.1146/annurev.biochem.75.062003.101730)

Jacobsen, E. N., Pfaltz, A. & Yamamoto, H. (eds) 1999 *Comprehensive asymmetric catalysis*, New York, NY: Springer.

Jenkins, D. M., Di Bilio, A. J., Allen, M. J., Betley, T. A. & Peters, J. C. 2002 Elucidation of a low spin cobalt(II) system in a distorted tetrahedral geometry. *J. Am. Chem. Soc.* **124**, 15 336–15 350. (doi:10.1021/ja026433e)

Jordan, A. & Reichard, P. 1998 Ribonucleotide reductases. *Annu. Rev. Biochem.* **67**, 71–98. (doi:10.1146/annurev.biochem.67.1.71)

Kang, S. O., Llinares, J. M., Powell, D., VanderVelde, D. & Bowman-James, K. 2003 New polyamide cryptand for anion binding. *J. Am. Chem. Soc.* **125**, 10 152–10 153. (doi:10.1021/ja034969+)

Kisker, C., Schindelin, H. & Rees, D. C. 1997 Molybdenum-cofactor-containing enzymes: structure and mechanism. *Annu. Rev. Biochem.* **66**, 233–267. (doi:10.1146/annurev.biochem.66.1.233)

Lewis, N. S. & Nocera, D. G. 2006 Powering the planet: chemical challenges in solar energy utilization. *Proc. Natl Acad. Sci. USA* **103**, 15 729–15 735. (doi:10.1073/pnas.0603395103)

Lieberman, R. L. & Rosenzweig, A. C. 2005 Crystal structure of membrane-bound metalloenzymes that catalyses the biological oxidation of methane. *Nature* **434**, 177–182. (doi:10.1038/nature03311)

Liu, S.-Y. & Nocera, D. G. 2005 Hangman salophens. *J. Am. Chem. Soc.* **127**, 5278–5279. (doi:10.1021/ja042849b)

Loll, B., Kern, J., Saenger, W., Zouni, A. & Biesiadka, J. 2005 Towards complete cofactor arrangement in the 3.0 Å resolution of photosystem II. *Nature* **438**, 1040–1044. (doi:10.1038/nature04224)

MacBeth, C. E., Golombek, A. P., Young Jr, V. G., Yang, C., Kuczera, K., Hendrich, M. P. & Borovik, A. S. 2000 O_2 activation by nonheme iron complexes: a monomeric Fe(III)-oxo complex derived from O_2. *Science* **289**, 938–941. (doi:10.1126/science.289.5481.938)

MacBeth, C. E., Gupta, R., Mitchell-Koch, K. R., Young Jr, V. G., Lushington, G. H., Thompson, W. H., Hendrich, M. P. & Borovik, A. S. 2004 Utilization of hydrogen bonds to stabilize M–O(H) units: synthesis and properties of monomeric iron and manganese complexes with terminal oxo and hydroxo ligands. *J. Am. Chem. Soc.* **126**, 2556–2567. (doi:10.1021/ja0305151)

Malmström, B. G. 1990 Cytochrome *c* oxidase as a redox-linked proton pump. *Chem. Rev.* **90**, 1247–1260. (doi:10.1021/cr00105a008)

McEvoy, J. P. & Brudvig, G. W. 2006 Water-splitting chemistry of photosystem II. *Chem. Rev.* **106**, 4455–4483. (doi:10.1021/cr0204294)

McHatton, R. C. & Anson, F. C. 1984 Electrochemical behavior of Ru(trpy)(bpy)$(OH_2)^{3+}$ in aqueous solution and when incorporated in nafion coatings. *Inorg. Chem.* **23**, 3935–3942. (doi:10.1021/ic00192a020)

Messinger, J., Badger, M. & Wydrzynski, T. 1995 Detection of one slowly exchanging substrate water molecule in the S_3 state of photosystem II. *Proc. Natl Acad. Sci. USA* **92**, 3209–3213. (doi:10.1073/pnas.92.8.3209)

Meunier, B., de Visser, S. P. & Shaik, S. 2004 Mechanism of oxidation reactions catalyzed by cytochrome P450 enzymes. *Chem. Rev.* **104**, 3947–3980. (doi:10.1021/cr020443g)

Müller, J. & Pindur, U. 1984 Reactions of electron-rich heterocycles with derivatives of carboxylic ortho acids, II: acid catalyzed reactions of 3-substituted indoles with ethyl orthoformates. *Arch. Pharm.* **317**, 555–561. (doi:10.1002/ardp.19843170612)

Newcomb, M. & Toy, P. H. 2000 Hypersensitive radical probes and the mechanisms of cytochrome P450-catalyzed hydroxylation reactions. *Acc. Chem. Res.* **33**, 449–455. (doi:10.1021/ar960058b)

Newcomb, M., Zhang, R., Chandrasena, R. E. P., Halgrimson, J. A., Horner, J. H., Makris, T. M. & Sligar, S. G. 2006 Cytochrome P450 compound I. *J. Am. Chem. Soc.* **128**, 4580–4581. (doi:10.1021/ja060048y)

Nocera, D. G. 2006 On the future of global energy. *Daedalus* **135**, 112–115. (doi:10.1162/daed.2006.135.4.112)

Odom, A. L. & Cummins, C. C. 1995 Nitric oxide cleavage: synthesis of terminal chromium(VI) nitride complexes via nitrosyl deoxygenation. *J. Am. Chem. Soc.* **117**, 6613–6614. (doi:10.1021/ja00129a034)

Pecoraro, V. L., Baldwin, M. J., Caudle, M. T., Hsieh, W. Y. & Law, N. A. 1998 A proposal for water oxidation in photosystem II. *Pure Appl. Chem.* **70**, 925–929.

Peloquin, J. M. & Britt, R. D. 2001 EPR/ENDOR characterization of the physical and electronic structure of the OEC Mn cluster. *Biochim. Biophys. Acta Bioenerg.* **1503**, 96–111. (doi:10.1016/S0005-2728(00)00219-X)

Que Jr, L. & Ho, R. Y. N. 1996 Dioxygen activation by enzymes with mononuclear non-heme iron active sites. *Chem. Rev.* **96**, 2607–2624. (doi:10.1021/cr960039f)

Reece, S. Y., Hodgkiss, J. M., Stubbe, J. & Nocera, D. G. 2006 Proton-coupled electron transfer: the mechanistic upderpinning for radical transport and catalysis in biology. *Phil. Trans. R. Soc. B* **361**, 1351–1364. (doi:10.1098/rstb.2006.1874)

Rieth, R. D., Mankad, N. P., Calimano, E. & Sadighi, J. P. 2004 Palladium-catalyzed cross-coupling of pyrrole anions with aryl chlorides, bromides, and iodides. *Org. Lett.* **6**, 3981–3983. (doi:10.1021/ol048367m)

Rosenthal, J., Chng, L. L., Fried, S. D. & Nocera, D. G. 2007 Stereochemical control of H_2O_2 dismutation by Hangman porphyrins. *Chem. Commun.* 2642–2644. (doi:10.1039/b616884a)

Rosenzweig, A. C. & Sazinsky, M. H. 2006 Structural insights into dioxygen-activating copper enzymes. *Curr. Opin. Struct. Biol.* **16**, 729–735. (doi:10.1016/j.sbi.2006.09.005)

Ruttinger, W. & Dismukes, G. C. 1997 Synthetic water-oxidation catalysts for artificial photosynthetic water oxidation. *Chem. Rev.* **97**, 1–24. (doi:10.1021/cr950201z)

Schrock, R. R. 1997 Transition metal complexes that contain a triamidoamine ligand. *Acc. Chem. Res.* **30**, 9–16. (doi:10.1021/ar950195t)

Sens, C., Romero, I., Rodriguez, M., Llobet, A., Parella, T. & Benet-Buchholz, J. 2004 A new Ru complex capable of catalytically oxidizing water to molecular dioxygen. *J. Am. Chem. Soc.* **126**, 7798–7799. (doi:10.1021/ja0486824)

Shaik, S., Kumar, D., De Visser, S. P., Altun, A. & Thiel, W. 2005 Theoretical perspective on the structure and mechanism of cytochrome P450 enzymes. *Chem. Rev.* **105**, 2279–2328. (doi:10.1021/cr030722j)

Shi, Y., Cao, C. & Odom, A. L. 2004 Synthesis and group 4 complexes of tris(pyrrolyl-α-methyl)amine. *Inorg. Chem.* **43**, 275–281. (doi:10.1021/ic035049v)

Siegbahn, P. E. M. 2006 O–O bond formation in the S_4 state of the oxygen-evolving complex in photosystem II. *Chem. Eur. J.* **12**, 9217–9227. (doi:10.1002/chem.200600774)

Solomon, E. I., Sundaram, U. M. & Machonkin, T. E. 1996 Multicopper oxidases and oxygenases. *Chem. Rev.* **96**, 2563–2605. (doi:10.1021/cr950046o)

Sono, M., Roach, M. P., Coulter, E. D. & Dawson, J. H. 1996 Heme-containing oxygenases. *Chem. Rev.* **96**, 2841–2887. (doi:10.1021/cr9500500)

Soper, J. D., Kryatov, S. V., Rybak-Akimova, E. V. & Nocera, D. G. 2007 Proton-directed redox control of O–O bond activation by heme hydroperoxidase models. *J. Am. Chem. Soc.* **129**, 5069–5075. (doi:10.1021/ja0683032)

Stubbe, J. & van der Donk, W. A. 1998 Protein radicals in enzyme catalysis. *Chem. Rev.* **98**, 705–762. (doi:10.1021/cr9400875)

Stubbe, J., Nocera, D. G., Yee, C. S. & Chang, M. C. Y. 2003 Radical initiation in the class I ribonucleotide reductase: long-range proton-coupled electron transfer? *Chem. Rev.* **103**, 2167–2201. (doi:10.1021/cr020421u)

Takeuchi, K. J., Thompson, M. S., Pipes, D. W. & Meyer, T. J. 1984 Redox and spectral properties of monooxo polypyridyl complexes of ruthenium and osmium in aqueous media. *Inorg. Chem.* **23**, 1845–1851. (doi:10.1021/ic00181a014)

Tommos, C. 2002 Electron, proton and hydrogen-atom transfers in photosynthetic water oxidation. *Phil. Trans. R. Soc. B* **357**, 1383–1394. (doi:10.1098/rstb.2002.1135)

Vrettos, J. S., Limburg, J. & Brudvig, G. W. 2001 Mechanism of photosynthetic water oxidation: combining biophysical studies of photosystem II with inorganic model chemistry. *Biochim. Biophys. Acta Bioenerg.* **1503**, 229–245. (doi:10.1016/S0005-2728(00)00214-0)

Wada, T., Tsuge, K. & Tanaka, K. 2001*a* Electrochemical oxidation of water to dioxygen catalyzed by the oxidized form of the bis(ruthenium-hydroxo) complex in H_2O. *Angew. Chem. Int. Ed.* **39**, 1479–1482. (doi:10.1002/(SICI)1521-3773(20000417)39:8<1479::AID-ANIE1479>3.0.CO;2-4)

Wada, T., Tsuge, K. & Tanaka, K. 2001*b* Syntheses and redox properties of bis(hydroxoruthenium) complexes

with quinone and bipyridine ligands: water-oxidation catalysis. *Inorg. Chem.* **40**, 329–337. (doi:10.1021/ic000552i)

Wallar, B. J. & Lipscomb, J. D. 1996 Dioxygen activation by enzymes containing binuclear non-heme iron clusters. *Chem. Rev.* **96**, 2625–2658. (doi:10.1021/cr9500489)

Watanabe, Y. 2000 High-valent intermediates. In *The porphyrin handbook*, vol. 4 (eds K. M. Kadish, K. M. Smith & R. Guilard), pp. 97–117. San Diego, CA: Academic Press.

Westphal, K. L., Tommos, C., Cukier, R. I. & Babcock, G. T. 2000 Concerted hydrogen-atom abstraction in photosynthetic water oxidation. *Curr. Opin. Plant Biol.* **3**, 236–242.

Whittaker, J. W. 2003 Free radical catalysis by galactose oxidase. *Chem. Rev.* **103**, 2347–2363. (doi:10.1021/cr020425z)

Wikström, M. 2004 Cytochrome *c* oxidase: 25 years of the elusive proton pump. *Biochim. Biophys. Acta* **1655**, 241–247. (doi:10.1016/j.bbabio.2003.07.013)

Yang, X. & Baik, M.-H. 2004 Electronic structure of the water-oxidation catalyst $[(bpy)_2(OH_x)RuORu(OH_y)(bpy)_2]^{z+}$: weak coupling between the metal centers is preferred over strong coupling. *J. Am. Chem. Soc.* **126**, 13 222–13 223. (doi:10.1021/ja0462427)

Yang, X. & Baik, M.-H. 2006 *cis,cis*-$[(bpy)_2Ru^{V}O]_2O^{4+}$ catalyzes water oxidation formally via *in situ* generation of radicaloid Ru^{IV}–$O^{\cdot}$. *J. Am. Chem. Soc.* **128**, 7476–7485. (doi:10.1021/ja053710j)

Yang, J. Y. & Nocera, D. G. 2007 Catalase and epoxidation activity of manganese salen complexes bearing two xanthene scaffolds. *J. Am. Chem. Soc.* **129**, 8192–8198. (doi:10.1021/ja070358w) ASAP article

Yang, J. Y., Bachmann, J. & Nocera, D. G. 2006 Hangman salen platforms containing two xanthene scaffolds. *J. Org. Chem.* **71**, 8706–8714. (doi:10.1021/jo0613075)

Yano, J. *et al.* 2006 Where water is oxidized to dioxygen: structure of the photosynthetic Mn_4Ca cluster. *Science* **314**, 821–825. (doi:10.1126/science.1128186)

Yeh, C.-Y., Chang, C. J. & Nocera, D. G. 2001 Hangman porphyrins for the assembly of a model heme water channel. *J. Am. Chem. Soc.* **123**, 1513–1514. (doi:10.1021/ja003245k)

Yoon, J. & Solomon, E. I. 2007 Electronic structures of exchange coupled trigonal trimeric Cu(II) complexes: spin frustration, antisymmetric exchange, pseudo-A terms, and their relation to O_2 activation in the multicopper oxidases. *Coord. Chem. Rev.* **251**, 379–400. (doi:10.1016/j.ccr.2006.04.012)

Zhang, W., Loebach, J. L., Wilson, S. R. & Jacobsen, E. N. 1990 Enantioselective epoxidation of unfunctionalized olefins catalyzed by (salen)manganese complexes. *J. Am. Chem. Soc.* **112**, 2801–2803. (doi:10.1021/ja00163a052)

Zong, R. & Thummel, R. P. 2005 A new family of Ru complexes for water oxidation. *J. Am. Chem. Soc.* **127**, 12 802–12 803. (doi:10.1021/ja054791m)

Discussion

C. Dismukes (*Princeton University, USA*). What type of ligand field is needed at the OEC Mn_4 site to create the $Mn^{V}=O$ species that you say could form?

D. Nocera. We have addressed this issue in detail in the paper accompanying the Discussion (§§2a and 3a). In short, an oxo of a Mn^{V} oxidation state would be supported by a tetragonal field and a d^2 electron count. For this situation, the Mn oxo triple bond would be of order three. For a Mn^{IV} oxo, our inclination is to expect radical character involving the oxo.

A. Aulauloo (*University of Paris-Sud, France*). Concerning the ligand design for the biscompartmental *cryptand*, once you generate Mn=O inside the cavities, don't you think it will attack the aromatic ring?

D. Nocera. Any practical catalysts for water oxidation will have to be stable and stand up to a highly active oxo core. It seems almost a paradox—the presence of a high-valent and reactive oxo in an environment rife with reducible moieties—i.e. the C–C and C–H bonds of a ligand framework. But these are the same moieties in proteins and enzymes, and many of these are oxidases whose function is derived from a reactive metal oxo. Biology overcomes this paradox in many ways. A metallocofactor will be fixed with its surrounding reactive bonds directed away from the metal oxo. Alternatively, the metal-oxo cofactor is sometimes insulated in a non-reactive shell (except for the site of substrate binding). And if this is still not enough, then as the participants of this Discussion certainly are familiar with, biology incorporates repair mechanisms. It may come as no surprise that the S_4 state of OEC is particularly damaging; thus the D1 protein is replaced every 30–60 min. Such repair mechanisms do not exist for synthetic catalytic active sites—but they will have to be 'designed' to ensure that catalysts can withstand the harsh oxidizing conditions of oxygen generation from water. This is a frontier area of research (along with the design of working catalysts!). Now to the specifics of the question….the cryptate (compound **5**) in my manuscript is designed with the idea of robustness in mind. The use of the carboxamide linker should render these ligands resistant to oxidation, thus avoiding ligand degradation by reactive oxygen intermediates. Of course, we may also need to worry about the CH bonds on the phenyl spacer. If this is a problem, we will have to teflonize the spacer and replace the reactive CH bonds with CF bonds.